Vid-SME: Membership Inference Attacks against Large Video Understanding Models

Qi Li Runpeng Yu Xinchao Wang[*]
National University of Singapore
{liqi, r.yu}@u.nus.edu xinchao@nus.edu.sg

Abstract

Multimodal large language models (MLLMs) demonstrate remarkable capabilities in handling complex multimodal tasks and are increasingly adopted in video understanding applications. However, their rapid advancement raises serious data privacy concerns, particularly given the potential inclusion of sensitive video content, such as personal recordings and surveillance footage, in their training datasets. Determining improperly used videos during training remains a critical and unresolved challenge. Despite considerable progress on membership inference attacks (MIAs) for text and image data in MLLMs, existing methods fail to generalize effectively to the video domain. These methods suffer from poor scalability as more frames are sampled and generally achieve negligible true positive rates at low false positive rates (TPR@Low FPR), mainly due to their failure to capture the inherent temporal variations of video frames and to account for model behavior differences as the number of frames varies. To address these challenges, we introduce Vid-SME (Video Sharma–Mittal Entropy), the first membership inference method tailored for video data used in video understanding LLMs (VULLMs). Vid-SME leverages the confidence of model output and integrates adaptive parameterization to compute Sharma–Mittal entropy (SME) for video inputs. By leveraging the SME difference between natural and temporally-reversed video frames, Vid-SME derives robust membership scores to determine whether a given video is part of the model's training set. Experiments on various self-trained and open-sourced VULLMs demonstrate the strong effectiveness of Vid-SME. Code is available here.

1 Introduction

Multimodal large language models (MLLMs) [1, 11, 26, 55] have received widespread attention from the AI community. By combining large language models (LLMs) with vision encoders, MLLMs gain the ability to perform a wide range of vision-language tasks [17, 64, 19, 21]. Recently, there has been growing interest in extending MLLMs to video understanding [63, 28, 30, 45], driven by their strong capabilities in processing visual information. However, the rapid development of video understanding LLMs (VULLMs) also raises critical concerns regarding data privacy leakage, as videos used for model training may contain sensitive content, such as personal recordings and surveillance footage, which could be memorized and unintentionally exposed by the models [5, 48, 61]. This highlights the severity of the problem, since early studies demonstrate that models' memorization of data can be maliciously exploited to conduct membership inference attacks (MIAs) [44, 4], where adversaries aim to determine whether a specific data sample was used during training. However, despite the booming development of VULLMs, efforts to address this issue significantly lags behind.

Recent studies have explored MIAs on LLMs and MLLMs [59, 43, 24, 50]. However, we observe that directly applying these methods to VULLMs results in extremely poor performance, and the

[*] Corresponding Author

39th Conference on Neural Information Processing Systems (NeurIPS 2025).

performance often deteriorates as more frames are introduced. The underlying reason is that these methods adopt a static view of MIA, which is inconsistent with the temporal nature and complex inter-frame variations of video data. Moreover, they overlook the intricate relationship between MIAs and model performance variations across different frame conditions. Since MIAs fundamentally rely on identifying model memorization [44] and such memorization in VULLMs may vary with the frame conditions [34, 56], the model tends to provide substantially different inference signals to the adversary when processing different number of frames from the same video. Therefore, successful MIAs on VULLMs generally require a video-specific and adaptive solution that takes into account both video statistics and performance fluctuations across different frame conditions.

In this work, we introduce Vid-SME (Video Sharma–Mittal Entropy), the first membership inference attack specifically devised to identify videos used in the training of VULLMs. Vid-SME leverages the flexible entropy formulation of Sharma–Mittal Entropy [42, 2, 14, 51] to adaptively capture the specific inter-frame variations of video frame sequences and compute customized entropy values. To account for different frame conditions, Vid-SME further exploits the model's behavioral differences between natural and reversed frame sequences to compute the final membership score. This design is motivated by our observation that, if a video was seen during training, the model tends to predict the next token with higher confidence when frames are presented in their natural order, leading to a lower entropy value. In contrast, when processing reversed frame sequences, the model exhibits more pronounced confidence degradation on seen videos, resulting in a more noticeable increase in entropy value. This ultimately yields a larger entropy gap between natural and reversed sequences for those seen videos, which serves as a strong membership signal.

We evaluate the performance of Vid-SME on various frame conditions, target datasets and target models. The results consistently demonstrate its strong effectiveness in inferring video membership in VULLMs. We summarize our contributions as follows:

- We introduce Vid-SME, the first dedicated method for video membership inference, which adaptively adjusts the controllable parameters in Sharma–Mittal entropy and leverages reversed frame sequences to capture the inherent temporal nature and complex inter-frame variations in videos, thus achieving reliable membership inference.
- Open-sourced VULLMs are commonly trained on multi-source datasets with only a portion of the training data publicly available, making it difficult to isolate the effects of task types and data distributions on MIA performance. To enable more controlled evaluation, we establish a benchmark by training three VULLMs, each on a distinct dataset, using two representative training strategies (Video-XL [45] and LongVA [63]).
- Extensive experiments across five VULLMs (three self-trained and two open-sourced) clearly demonstrate the superiority of Vid-SME. For example, when applied to the open-sourced LLaVA-NeXT-Video-34B [27, 65], Vid-SME delivers a 28.3% improvement in AUC, an 18.1% increase in accuracy, and an impressive 293% boost in TPR@5% FPR.

2 Related Work

2.1 MultiModal Large Language Models

Building on the success of large language models (LLMs) [12, 13, 36, 52], multimodal large language models (MLLMs) [1, 11, 26, 55] integrate visual encoders to extract visual features, which are then aligned to the same dimensional space as LLM tokens through dedicated connectors, enabling effective visual-language processing. Recent advancements in MLLMs have led to significant improvements in image-related tasks. Video Understanding Large Language Models (VULLMs) [63, 28, 45, 30] further expand the capabilities of MLLMs to video understanding by encoding multi-frame features and concatenating them for uniform interpretation. The typical working pipeline of VULLMs for video data closely follows that of image-based MLLMs [30, 28]. For example, a visual encoder is usually employed to extract spatiotemporal features from videos. These features are then projected into the input space of the large language model through a learnable linear projection layer, enabling seamless integration with language tokens.

VULLMs commonly adapt pretrained image-based MLLMs for video tasks [33, 45, 63, 32, 37], which are usually trained on image and text modalities and then instruction-tuned on carefully designed video instruction data, during which only the linear projection layer is updated, while the rest of the architecture remains frozen [32]. Recent efforts, including LongVA [63], Video-XL [45], and the LLaVA-NeXT-Video series [27, 65], focus on enhancing temporal modeling to support long video comprehension, and have demonstrated strong performance on related tasks.

2.2 Membership Inference Attack

Membership Inference Attacks (MIAs) [44, 4, 23, 54] aim to determine whether a specific data sample was included in a model's training set. For a machine learning model, ensuring the confidentiality of its training data is critical, as it may contain sensitive or personal information about individuals. Existing MIA methods can be broadly categorized into two types [4, 24]: metric-based and shadow model-based. Metric-based MIAs [59, 40, 49, 24] rely on evaluating certain metrics derived from the target model's outputs and making membership decisions based on predefined thresholds. In contrast, shadow model-based MIAs [44, 60] train additional models to replicate the behavior of the target model, which requires extensive computational resources and is often impractical for LLMs [24]. Thus, this work focuses exclusively on metric-based methods.

MIAs were initially applied in the context of classification models [44], but have since been extended to other types of models, such as generative models [10, 18] and embedding models [31, 47]. With the rapid advancement of LLMs and MLLMs, researchers have begun to explore the feasibility of conducting MIAs against these models as well. For example, [43] proposed Min-$K\%$, which selects the smallest $K\%$ of probabilities corresponding to the ground-truth token, while [24] argued that detecting individual images or texts is more practical in real-world scenarios and presents additional challenges. To address this, they introduced MaxRényi-$K\%$ and its variant version ModRényi, investigating the potential for extracting and attacking unimodal information from MLLMs. However, to the best of our knowledge, no existing work has explored the privacy risks of MIAs on video understanding large language models (VULLMs).

In addition, existing MIA studies on (M)LLMs can generally be categorized into those targeting pretraining data [43, 62, 8] and those targeting instruction tuning data [24, 57, 20]. Unlike these models, as dicussed in Section 2.1, VULLMs are commonly built by adapting image-based MLLMs to video tasks [33, 45, 63, 32, 37]. These models are initially trained on image–text data and instruction-tuned using video instruction datasets. As a result, MIAs against videos in VULLMs are primarily constrained to the instruction tuning stage. This highlights the unique importance of this problem: The capability of VULLMs to effectively interact with humans fundamentally depends on the instruction tuning stage, as the strength of this capability is directly tied to the quality of the instruction tuning dataset. Furthermore, developers often construct their own task-specific datasets for this stage [45, 63, 22], which introduces additional privacy risks. Motivated by these factors, our work focuses on video membership inference during the instruction tuning stage of VULLMs.

3 Problem Setting and Challenges

Notation. The token set is denoted by $\mathcal{V}$. A sequence of L tokens is denoted as $X := (x_1, x_2, \ldots, x_L)$, where $x_k \in \mathcal{V}$ for $k \in [L]$. Let $X_1 \| X_2$ denote the aggregation of sequences X_1 and X_2. A video token sequence is denoted as $F_{1:T}$, where T represents the number of frames. In this work, we focus on a VULLM f_θ, parameterized by θ, where the input of the model consists of $F_{1:T}$ and an instruction context X_{ins}, and the output is the response text X_{res}. We use $\mathcal{D}_{\text{vid}}$ to represent the video set containing the videos used in model training.

Adversary's Goal. We follow the standard definition of MIAs as described in [44]. Given a VULLM f_θ, the adversary aims to determine whether a specific video was used during the instruction tuning stage of f_θ. We formulate this attack as a binary classification problem. Let $\mathbf{A}(F_{1:T};\theta) :\rightarrow \{0,1\}$ denote the membership detector. During the attack, we feed the model with $F_{1:T}$ and the instruction context X_{ins}. The membership detector makes its decision by comparing a metric $I(F_{1:T} \oplus X_{\text{ins}};\theta)$ with a certain threshold λ:

$$\mathbf{A}(F_{1:T};\theta) = \begin{cases} 1 & (F_{1:T} \in \mathcal{D}_{\text{vid}}), \text{ if } I(F_{1:T} \| X_{\text{ins}};\theta) < \lambda, \\ 0 & (F_{1:T} \notin \mathcal{D}_{\text{vid}}), \text{ if } I(F_{1:T} \| X_{\text{ins}};\theta) \geq \lambda. \end{cases} \tag{1}$$

Adversary's Knowledge. Following the standard MIA setup [24, 57], we assume a grey-box scenario where the adversary can query the target model using the video frames and the instruction context,

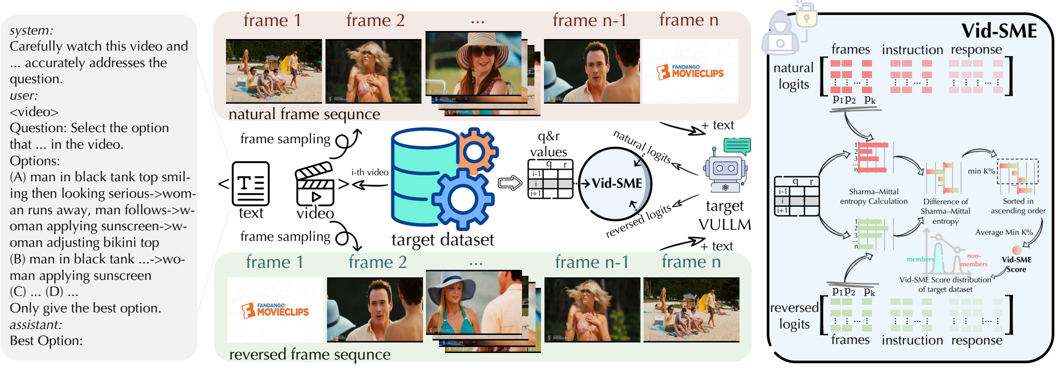

system:
Carefully watch this video and ... accurately addresses the question.
user:
<video>
Question: Select the option that ... in the video.
Options:
(A) man in black tank top smiling then looking serious->woman runs away, man follows->woman applying sunscreen->woman adjusting bikini top
(B) man in black tank ...->woman applying sunscreen
(C) ... (D) ...
Only give the best option.
assistant:
Best Option:

Figure 1: Vid-SME against VULLMs. **Left:** An example of the video instruction context used in our experiments. **Middle:** The overall pipeline of Vid-SME. **Right:** The detailed illustration of the membership score calculaiton of Vid-SME.

and is allowed to access the tokenizer, output logits, and generated text. However, the adversary has no knowledge of the training algorithm or the model parameters of the target model.

Challenges. (i). Unlike conventional LLMs and image-based MLLMs, VULLMs incorporate video modality during instruction tuning, enabling multimodal understanding beyond static images and text. The temporal nature and complex inter-frame variations inherent in video data makes membership inference significantly more challenging. **(ii).** Membership inference fundamentally relies on the model's memorization of training data [44]. However, memorization in LLMs is generally weak. This becomes more subtle for video data, where the number of frames fed into VULLMs can influence the model performance and thus influence the degree of memorization [34, 56]. The variation in the frame conditions makes the relationship between the attack performance and the model's memorization highly intricate, thereby posing additional challenges for effective attacks. **(iii).** On the dataset side, video instruction tuning data for VULLMs typically comes from diverse and heterogeneous sources [63, 45, 65], leading to highly complex data distributions. Moreover, it is often difficult to find non-member data that shares a similar distribution with the training set. Previous MIAs on text and image data attempt to synthesize non-member samples using LLMs or image generation models [24], whereas such synthesis remains challenging for video data. The distribution shift between members and non-members poses additional challenges for the evaluation of membership inference.

4 Method

Similar to image-based MLLMs, VULLMs also usually project the vision encoder's embedding of the video frame sequence into the feature space of LLM. Under the grey-box setting, intermediate information from the LLM is inaccessible, and gradient-based operations (e.g., backpropagation) cannot be performed. To this end, we propose a token-level video MIA that computes metrics based on the output logits at each token position.

Figure 1 illustrates the full pipeline of our proposed attack, which can be divided into three main stages: data preprocessing, model inference, and membership inference. In the data preprocessing stage, we perform frame sampling on all videos in the target dataset containing members and non-members. Without loss of generality, we adopt uniform sampling based on frame indices. Additionally, to capture the specific inter-frame variations of each video frame sequence, we customize the order parameter q and deformation parameter r of Sharma–Mittal Entropy [42] by incorporating the video's motion complexity and illumination variation into their determination. In the model inference stage, the sampled video frames and the instruction context are fed into the target VULLM. This step is conducted twice, using both the natural frame order and the reversed frame order, respectively. Finally, in the membership inference stage, we extract the slices of natural and reversed logits corresponding to the video frames, which can be easily located based on the model's special tokens [24]. Using the customized q and r values, we compute the Sharma–Mittal entropy for both slices, and derive the final membership score through the differences between the two entropy values.

Sharma–Mittal entropy. Sharma-Mittal entropy is one of the entropy metrics that is widely used in information theory and statistical learning due to its flexibility [42, 14, 51]. It allows for tunable sensitivity to different regions of a probability distribution, which is particularly beneficial in scenarios involving complex distributions such as those observed in video-language modeling and membership inference attacks. It generalizes several well-known entropy formulations and can be defined as $S_{q,r}(p) = \frac{1}{1-r}\left(\left(\sum_j p_j^q\right)^{\frac{1-r}{1-q}} - 1\right), q, r \in (0, \infty) \setminus \{1\}$, where $p = \{p_j\}$ represents a probability distribution, and q and r are two adjustable parameters that control the entropy's sensitivity and aggregation behavior, respectively. The parameter q determines how the entropy responds to the skewness of the distribution. Specifically, smaller values of q increase sensitivity to low-probability (rare) events, while larger values of q emphasizes more on high-probability (dominant) modes. In contrast, r governs the nonlinearity and aggregation scheme in entropy calculation. Larger values of r make the entropy calculation more nonlinear, thereby increasing its sensitivity to distribution peaks.

4.1 Adaptive Parameterization

Videos naturally exhibit highly diverse visual properties. Such diversity impacts the model's prediction distributions. For instance, fast-moving videos with large inter-frame variations often induce higher uncertainty, leading to more dispersed predictions, while stable videos result in more confident and concentrated outputs [35, 16, 67, 3]. Moreover, videos with obvious illumination variations may introduce abnormal prediction fluctuations, as sudden brightness changes can create misleading visual cues that confuse the model and cause it to overly favor certain tokens [9, 58, 46, 29]. Thus, algin with the properties of Sharma–Mittal entropy, we adapt the parameters q and r for each video frame sequence based on its motion complexity and illumination variation.

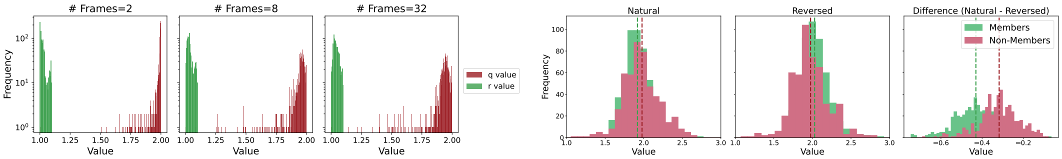

(a) Variation of q/r values with respect to # frames. (b) Natural-reversed entropy difference is essential.

Figure 2: Example of the q/r value distribution and entropy distribution on Video-XL-CinePile-7B.

To do so, for the i-th video, after the frame sequence sampling, we quantify its motion complexity ϕ_i as the mean variance of optical flow [15] between consecutive frames, while its illumination variation λ_i is measured as the standard deviation of average brightness across frames. Specifically, each frame is first converted to grayscale, and the mean brightness of each frame is computed; the standard deviation of these mean values then reflects the overall illumination variation within the sequence. Both statistics are further normalized in the target dataset to obtain normalized statistics $\hat{\phi}_i$ and $\hat{\lambda}_i$, respectively. The entropy parameters q_i and r_i of the i-th video are then determined as:

$$q_i = 1 + \beta_1 \cdot \frac{\max_j \hat{\phi}_j - \hat{\phi}_i}{\max_j \hat{\phi}_j - \min_j \hat{\phi}_j}, \quad r_i = 1 + \beta_2 \cdot \frac{\hat{\lambda}_i - \min_j \hat{\lambda}_j}{\max_j \hat{\lambda}_j - \min_j \hat{\lambda}_j}, \tag{2}$$

where β_1 and β_2 are scaling coefficients controlling the adjustment range of each parameter, which are set to 1.0 and 0.1, respectively, to better align with the nature of Sharma-Mittal entropy calculation. In this design, video frame sequences with higher motion complexity (i.e., larger ϕ) are assigned smaller q values, as higher motion typically leads to more uncertain predictions, resulting in flatter probability distributions with more low-probability tokens. Smaller q values increase the sensitivity of the entropy calculation to these low-probability tokens, thus better reflecting the model's uncertainty in such cases. Meanwhile, videos with larger illumination variations (i.e., larger λ) are assigned larger r values, which enhances the nonlinearity of the entropy calculation and increases its sensitivity to abnormal predictions.

4.2 Vid-SME

We now propose our Vid-SME, utilizing the Sharma–Mittal entropy of the next-token probability distribution. Specifically, given a token sequence $X := (x_1, x_2, \dots, x_L)$ consisting of video frame tokens and instruction context tokens (i.e., $X = F_{1:T} \| X_{\text{ins}}$), let $p_k(\cdot) = \mathcal{P}(\cdot | x_1, \dots, x_k; \theta)$ be the next-token probability distribution at the k-th position. We then extract the video-related probability slices, denoted by $\bar{p}_{1:T} = \{p_k(\cdot) \mid x_k \in F_{1:T}\}$. Accordingly, the video-related probability slices corresponding to the reversed video sequence can be extracted, denoted as $\bar{p}_{T:1} = \{\hat{p}_k(\cdot) \mid x_k \in F_{T:1}\}$, where $F_{T:1}$ denotes the reversed video token sequence, $\hat{p}_k(\cdot)$ is the next-token probability distribution for the reversed video sequence at the k-th position. The Sharma-Mittal entropy is then computed for the natural and reversed probability slices, resulting in

$$S_{\text{nat}} = \{S_{q,r}\left(p_k(\cdot)\right) \mid p_k(\cdot) \in \bar{p}_{1:T}\}\,, \quad S_{\text{rev}} = \{S_{q,r}\left(\hat{p}_k(\cdot)\right) \mid \hat{p}_k(\cdot) \in \bar{p}_{T:1}\}\,, \tag{3}$$

where $S_{q,r}(\cdot)$ denotes the Sharma-Mittal entropy with adaptively determined parameters q and r. After that, we calculate the element-wise differences between the two sequences as $\Delta S^{(\xi)} = S_{\text{nat}}^{(\xi)} - S_{\text{rev}}^{(\xi)}$, for $\xi = 1, 2, \ldots, |S_{\text{nat}}|$. Let Min-$K\%(\Delta S)$ be the smallest $K\%$ from the sequence ΔS. The final Vid-SME score for current video frame sequence is computed as

$$\texttt{Vid-SME-K\%}(F_{1:T}) = \frac{1}{|\text{Min-}K\%(\Delta S)|} \sum_{\xi \in \text{Min-}K\%(\Delta S)} \Delta S^{(\xi)}. \tag{4}$$

When $K = 0$, the `Vid-SME-K%` score is defined to be $\min_{\xi} \Delta S^{(\xi)}$. When $K = 100$, the `Vid-SME-K%` score is the mean $\Delta S^{(\xi)}$ value of the sequence $F_{1:T}$. As $q \to 1$, the formulation of Sharma-Mittal entropy reduces to the classical Shannon entropy [41]; when $r \to 1$, Sharma-Mittal entropy reduces to Rényi entropy [39]; when $r = q$, it corresponds to Tsallis entropy [53]. Formal definitions of these simpler form can be found in Appendix F. In practice, we set a sufficiently small threshold of 1×10^{-10}. When the different between q and 1, r and 1, or between q and r falls below this threshold, the entropy calculation in Vid-SME degenerates into the corresponding simpler form.

The variation of q/r values with respect to the number of sampled frames. As shown in Figure 2a, increasing the number of frames makes the q/r values more video-specific, suggesting that the richer video information brought by additional frames is effectively reflected in the q/r values.

The significance of the natural-reversed entropy difference. As shown in Figure 2b, while the natural and reversed entropy distributions offer some separation between members and non-members, they are insufficient for clear discrimination. In contrast, the natural-reversed entropy difference significantly amplifies the distribution gap, making the distinction much more pronounced.

5 Experiments

Datasets and Models. To comprehensively evaluate the attack performance, we construct member and non-member sets for five target models, including three self-trained models, covering various task types, video lengths, and dataset scales. The details of these datasets are summarized in Table 1. The configurations and training trajectories of the three self-trained models are given in Appendix A.

Specifically, we follow the training pipeline and model components of Video-XL-7B [45] and instruction tune the model on two distinct datasets to obtain Video-XL-NExT-QA-7B and Video-XL-CinePile-7B, respectively. NExT-QA [25] is a video question answering dataset while CinePile [38] is a video order reasoning dataset. For the NExT-QA dataset, we randomly sample 1070, 2140, and 4280 instances from both the training and testing splits to construct the member and non-member sets, respectively. This results in target datasets with three different scales (i.e., 2140, 4280 and 8560). Unless otherwise specified, we default to using 2140 instances for both members and non-members (4280 in total) in all the experiments. Results under different dataset scales are reported in Table 4. For Video-XL-CinePile-7B, the non-member set consists of all 502 instances from nine scenarios in the MLVU benchmark [66], which involve sequential reasoning tasks similar to CinePile. To ensure consistency in scale, we randomly sample 502 videos from CinePile as the member set. In addition to these, we follow the training pipeline and model components of LongVA [63] and instruction tune the model with video captioning data from Video-XL training set [45] to obtain LongVA-Caption-7B. We use all the 1027 samples from the detailed captioning category in the VDC benchmark [7] as the non-member set and randomly sample 1027 instances from the model's training set as members.

Target Model	Member Data				Non-Member Data			
	source	scale	duration(s)	fps	source	scale	duration(s)	fps
Video-XL-NExTQA-7B	NExT-QA [25]	1070 2140 4280	45.22 46.01 44.68	28.89 28.84 28.77	NExT-QA [25]	1070 2140 4280	39.17 36.52 38.91	28.75 28.73 28.68
Video-XL-CinePile-7B	CinePile [38]	502	159.80	23.98	MLVU [66]	502	933.66	29.05
LongVA-Caption-7B	Video-XL [45]	1027	24.18	28.29	VDC [7]	1027	30.07	28.57
LLaVA-NeXT-Video-7B/34B	Video-Instruct-100K [32]	869	116.57	25.03	Video-XL [45]	869	24.79	28.02

Table 1: Statistics of datasets for each target VULLM.

Beyond our self-trained models, we also include two open-sourced models for evaluation: LLaVA-NeXT-Video-7B [65] and LLaVA-NeXT-Video-34B [65]. For these models, we use the video

Metric		Video-XL-NExT-QA-7B [45]			Video-XL-CinePile-7B [45]			LongVA-Caption-7B [63]			LLaVA-NeXT-Video-7B [65, 27]			LLaVA-NeXT-Video-34B [65, 27]		
		AUC	Acc.	TPR@5% FPR	AUC	Acc.	TPR@5% FPR	AUC	Acc.	TPR@5% FPR	AUC	Acc.	TPR@5% FPR	AUC	Acc.	TPR@5% FPR
Perplexity		0.461	0.502	0.048	0.679	0.667	0.004	0.497	0.527	0.028	0.388	0.501	0.002	0.379	0.505	0.007
Max_Prob_Gap		0.497	0.521	0.050	0.543	0.559	0.020	0.507	0.521	0.049	0.480	0.514	0.020	0.286	0.502	0.014
Modified_Entropy		0.460	0.503	0.048	0.677	0.664	0.004	0.500	0.529	0.028	0.384	0.501	0.002	0.376	0.504	0.006
Min_0% Prob		0.482	0.515	0.028	0.500	0.544	0.006	0.474	0.501	0.034	0.271	0.501	0.000	0.417	0.500	0.016
Min_5% Prob		0.472	0.507	0.052	0.564	0.582	0.004	0.496	0.526	0.024	0.317	0.502	0.002	0.462	0.508	0.016
Min_30% Prob		0.469	0.508	0.062	0.619	0.622	0.004	0.510	0.529	0.033	0.344	0.501	0.003	0.440	0.508	0.014
Min_60% Prob		0.460	0.504	0.038	0.654	0.641	0.004	0.504	0.527	0.027	0.364	0.501	0.002	0.407	0.505	0.008
Min_90% Prob		0.461	0.502	0.048	0.680	0.666	0.004	0.497	0.528	0.028	0.383	0.501	0.002	0.382	0.505	0.007
ModRényi	$\alpha = 0.5$	0.460	0.504	0.046	0.694	0.685	0.006	0.497	0.526	0.025	0.398	0.501	0.002	0.358	0.503	0.007
	$\alpha = 2$	0.460	0.501	0.040	0.703	0.688	0.006	0.494	0.524	0.030	0.411	0.501	0.002	0.341	0.504	0.007
Rényi ($\alpha = 0.5$)	Max_0%	0.457	0.502	0.036	0.589	0.616	0.010	0.521	0.528	0.032	0.262	0.500	0.007	0.378	0.500	0.010
	Max_5%	0.466	0.508	0.034	0.567	0.611	0.000	0.540	0.546	0.037	0.297	0.501	0.009	0.458	0.511	0.013
	Max_30%	0.463	0.511	0.050	0.575	0.602	0.002	0.538	0.547	0.046	0.251	0.501	0.006	0.555	0.557	0.052
	Max_60%	0.462	0.512	0.040	0.583	0.602	0.006	0.535	0.542	0.036	0.233	0.500	0.002	0.590	0.586	0.045
	Max_90%	0.469	0.507	0.052	0.607	0.617	0.006	0.496	0.503	0.044	0.250	0.500	0.000	0.585	0.588	0.044
Rényi ($\alpha = 1$)	Max_0%	0.450	0.501	0.024	0.538	0.579	0.004	0.506	0.522	0.028	0.360	0.500	0.007	0.383	0.500	0.012
	Max_5%	0.468	0.510	0.034	0.511	0.573	0.000	0.508	0.533	0.032	0.437	0.501	0.014	0.468	0.514	0.012
	Max_30%	0.468	0.509	0.056	0.563	0.594	0.000	0.530	0.538	0.038	0.312	0.500	0.001	0.518	0.546	0.025
	Max_60%	0.461	0.506	0.048	0.593	0.608	0.004	0.533	0.543	0.036	0.290	0.500	0.001	0.502	0.543	0.024
	Max_90%	0.460	0.506	0.044	0.623	0.620	0.000	0.514	0.533	0.037	0.319	0.500	0.001	0.479	0.533	0.021
Rényi ($\alpha = 2$)	Max_0%	0.470	0.505	0.012	0.479	0.553	0.002	0.484	0.502	0.035	0.315	0.500	0.004	0.403	0.500	0.010
	Max_5%	0.470	0.506	0.040	0.528	0.580	0.000	0.494	0.523	0.023	0.376	0.503	0.004	0.461	0.511	0.013
	Max_30%	0.468	0.510	0.062	0.591	0.597	0.002	0.515	0.532	0.036	0.341	0.501	0.001	0.465	0.520	0.016
	Max_60%	0.460	0.504	0.052	0.630	0.631	0.002	0.508	0.529	0.029	0.348	0.500	0.001	0.438	0.512	0.012
	Max_90%	0.460	0.503	0.052	0.661	0.655	0.004	0.499	0.531	0.028	0.371	0.500	0.002	0.416	0.508	0.010
Rényi ($\alpha = \infty$)	Max_0%	0.482	0.515	0.028	0.500	0.544	0.006	0.474	0.501	0.034	0.271	0.501	0.000	0.417	0.500	0.016
	Max_5%	0.472	0.507	0.052	0.564	0.582	0.004	0.496	0.526	0.024	0.317	0.502	0.002	0.462	0.508	0.016
	Max_30%	0.469	0.508	0.062	0.619	0.622	0.004	0.510	0.529	0.033	0.344	0.501	0.004	0.440	0.508	0.014
	Max_60%	0.460	0.504	0.038	0.654	0.641	0.004	0.504	0.527	0.027	0.364	0.501	0.002	0.407	0.505	0.008
	Max_90%	0.461	0.502	0.048	0.680	0.666	0.004	0.497	0.528	0.028	0.383	0.501	0.002	0.382	0.505	0.007
Vid-SME (Ours)	Mean	0.535	0.540	0.104	0.840	0.769	0.420	0.496	0.510	0.039	0.484	0.509	0.050	0.513	0.525	0.063
	Min_0%	0.519	0.528	0.030	0.559	0.568	0.114	0.544	0.545	0.056	0.490	0.509	0.050	0.757	0.692	0.204
	Min_5%	0.543	0.555	0.044	0.624	0.612	0.088	0.556	0.561	0.043	0.550	0.555	0.054	0.726	0.682	0.109
	Min_30%	0.545	0.547	0.074	0.699	0.670	0.161	0.541	0.553	0.050	0.601	0.579	0.073	0.696	0.654	0.102
	Min_60%	0.548	0.545	0.084	0.765	0.709	0.243	0.544	0.548	0.053	0.596	0.572	0.077	0.673	0.632	0.117
	Min_90%	0.538	0.541	0.106	0.830	0.765	0.305	0.538	0.550	0.035	0.523	0.531	0.058	0.597	0.577	0.092

Table 2: Results of Vid-SME and baseline methods when # frames=16. We highlight the best, second-best, and third-best results in progressively lighter shades of red, while marking the worst, second-worst, and third-worst results in progressively lighter shades of green.

caption dataset Video-Instruct-100K [32] that serves as part of their training data as the member set. Each video in this dataset has multiple questions, from which we select the one with the longest text length, resulting in 869 samples. The non-member set consists of 869 samples randomly selected from the captioning data from Video-XL training set [45].

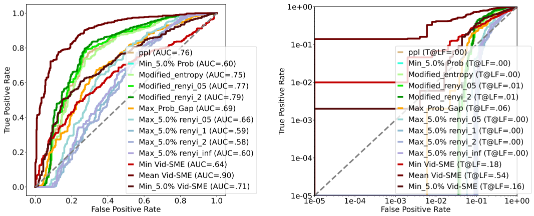

ROC

TPR@5% FPR

Figure 3: The ROC and TPR@5% FPR curves.

Baselines. We adopt several metric-based MIAs as baselines and compare them with Vid-SME. Specifically, we include the Loss attack [59], which corresponds to perplexity in the context of language models. We also involve the Min-$K\%$ method [43], which computes the smallest $K\%$ probabilities associated with the ground-truth tokens. We evaluate K values of 0, 5, 30, 60, and 90. In addition, we adopt the Max_Prob_Gap metric [24], which captures the model's confidence by computing the difference between the maximum and the second-largest probability at each token position, followed by averaging across the sequence. We further include MaxRényi-$K\%$ and its modified variant ModRényi proposed in [24], which are specifically designed for membership inference on image-based MLLMs and utilize the Rényi entropy of next-token probability distributions. For MaxRényi-$K\%$, we set α to 0.5, 1, 2, and ∞, while for ModRényi, we use α values of 0.5 and 2. We also include Modified Entropy [50] as our baseline, as it is a special case of ModRényi when $\alpha \to 1$.

Evaluation metric. As a binary classification problem, the performance can be evaluated with the AUC score [6]. We define the members as "positive" and the non-members as "negative". We also report True Positive Rate (TPR) at low False Positive Rate (FPR) [4], which is an important metric in MIAs and measures detection rate at a meaningful threshold. We set the threshold as 5% and evaluate all the methods under TPR@5% FPR. We also report the best classification accuracy achievable by sweeping over all possible thresholds on the attack scores. Specifically, this accuracy is computed as

# frames	Train-Test Gap
2	11.35
4	11.16
8	10.95
16	8.57
32	10.20

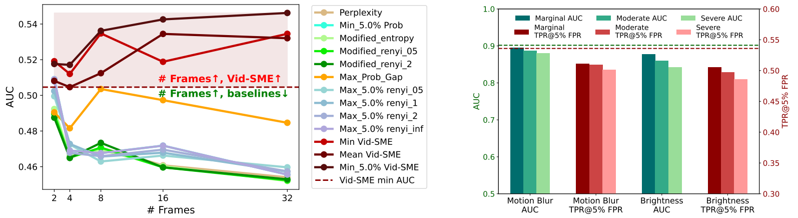

(a) Performance gap v.s. # frames.

(b) Attack performance (AUC) of different methods v.s. # frames.

(c) AUC and TPR@5% FPR under different corruptions.

Figure 4: Analysis on: (a) Train-Test Gap v.s. # frames, (b) Attack performance v.s. # frames, (c) Attack performance under different corruption types and levels.

the maximum value of $1 - \frac{\text{FPR}+(1-\text{TPR})}{2}$ across the ROC curve, representing the optimal classification accuracy between members and non-members. We use # frames to denote the number of frames.

5.1 Main Results

The experimental results across the five target VULLMs are summarized in Table 2. We highlight the best, second-best, and third-best results in progressively lighter shades of red, while marking the worst, second-worst, and third-worst results in progressively lighter shades of green. The # frames is fixed to 16. It can be observed that Vid-SME consistently achieves the best performance under all settings, especially excelling in the most critical metric, TPR@5% FPR. When the target VULLMs are Video-XL-CinePile-7B and LLaVA-NeXT-Video-7B, all baseline methods exhibit extremely low TPR@5% FPR values (around 0.001), which are impractically low for reliable membership inference. In contrast, Vid-SME consistently maintains TPR@5% FPR above 0.05 in these challenging scenarios, demonstrating remarkable improvements. In addition, the fact that baseline methods achieve AUC scores both above and below 0.5 across different settings indicates their inconsistency in distinguishing members from non-members. This suggests that they cannot serve as a reliable and unified indicator for membership inference in video-based scenarios.

Method	Ins. Type	Metric		
		AUC	Acc.	TPR@5% FPR
Perplexity	I_1	0.377	0.504	0.009
	I_2	0.406	0.509	0.002
	I_3	0.425	0.515	0.012
Max_Prob_Gap	I_1	0.287	0.500	0.012
	I_2	0.319	0.502	0.010
	I_3	0.346	0.501	0.009
Modified_Entropy	I_1	0.375	0.503	0.008
	I_2	0.403	0.509	0.004
	I_3	0.421	0.515	0.008
Min_5.0% Prob	I_1	0.448	0.506	0.021
	I_2	0.419	0.508	0.015
	I_3	0.429	0.508	0.020
Modified_Rényi ($\alpha = 0.5$)	I_1	0.357	0.503	0.008
	I_2	0.391	0.506	0.008
	I_3	0.412	0.512	0.010
Max_5.0% Rényi ($\alpha = 0.5$)	I_1	0.452	0.506	0.024
	I_2	0.422	0.509	0.016
	I_3	0.422	0.505	0.012
Min_5.0% Vid-SME	I_1	0.692	0.651	0.104
	I_2	0.714	0.664	0.100
	I_3	0.729	0.683	0.109

Table 3: Performance comparison on different instructions.

To be more intuitive, we illustrate the detailed comparisons for Video-XL-CinePile-7B with K = 0, 5, 100 in Figure 3, which presents both ROC and TPR@5% FPR curves. Among all methods, Vid-SME variants (K = 0, 5, 100) consistently achieve superior performance. Notably, Vid-SME-100% reaches the highest AUC of 0.90, substantially surpassing other baselines. Additionally, Vid-SME-0% and Vid-SME-100% achieve significantly higher TPR@5% FPR (0.18 and 0.54), while most baseline methods yield almost negligible performance (close to 0.0).

Relationship between model memorization, frame conditions and attack performance. To analyze the relationship among model memorization, frame conditions, and attack performance, we further investigate how the train-test performance gap and attack performance change under different frame counts (# frames). Results for Video-XL-NExT-QA-7B are given in Table 4a and Figure 4b. We can observe that, when # frames are limited, the model remains uncertain on both training and test samples, leading to poor generalization but also weak memorization. Thus, although the performance gap is large, attacks are less effective as explicit memorization has not yet emerged. As # frames increase, improved understanding of video content narrows the gap, but exploitable confidence differences between members and non-members arise, enhancing the attack effectiveness. With even more frames, the model becomes highly confident on training samples while struggling with distribution shifts or increased complexity in unseen test samples, which enlarges the gap and further amplifies train-test prediction differences, making attacks highly effective. This phenomenon highlights the non-linear relationship between memorization and MIA vulnerability in the context of VULLMs.

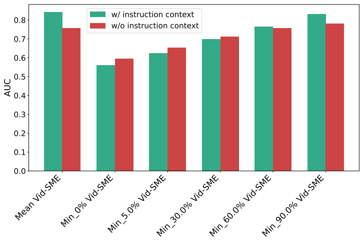

Figure 5: A comparison between with and without full context.

5.2 Ablation Study

Inflenuce of instruction context. We now refer to the instruction context used in our main experiments as I_1. To explore the influence of instruction context, we design two alternative contexts, denoted as I_2 and I_3. The details of $I_{1,2,3}$ are provided in Appendix C. The results when # frames = 8 and the target model is LLaVA-NeXT-Video-34B are reported in Table 3. As shown, the impact of the contexts is not significant. Furthermore, we observe that Vid-SME is less sensitive to context variations compared to other baselines, indicating better stability in its attack effectiveness.

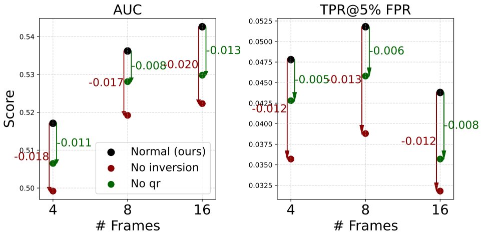

Figure 6: A comparison between with and without full instructions.

Furthermore, we investigate the scenario where text provides minimal information, and video frames are combined with only a short query text before being fed into the model, which makes the attack results independent of video-related understanding tasks. The short query text used here can be found in Appendix C. The results under this setting, using Video-XL-CinePile-7B as the target model and # frames = 8, are reported in Figure 5. It can be observed that when the selection range of ΔS is small (e.g., K = 0, 5, 30), attacks using only the short query text outperform those using the full instruction context. However, as the selection range of ΔS becomes more representative of the overall video probabilities (i.e., $K \uparrow$), the attack performance with the full instruction context gradually surpasses that of the short query text. This observation aligns with intuition: when the prediction probabilities for video-related tokens are shaped by rich task-specific textual context, the model's response generation becomes more strongly grounded in the video frames, increasing its reliance on the complete visual information. Overall, however, the performance difference between the two is not substantial.

Importance of q/r adaptation and reverse frame sequence. We further present the results when disabling the adaptive q/r values (No qr) and when removing the reversed frame sequence when calculating the membership score (No inversion). For the former, we assign fixed q and r values (i.e., $q = 2.0$, $r = 1.0$) across the entire target dataset. For the latter, instead of using ΔS, we directly adopt S_{nat} to compute the final membership score. The target model in this experiment is Video-XL-NExT-QA-7B, and we report the Vid-SME-5% results. As shown in Figure 6, removing either component leads to a significant performance drop, demonstrating the critical role of q/r adaptation and reversed frame sequence in performing membership inference attacks against VULLMs.

Method	# Frames	Dataset Scale	Metric		
			AUC	Acc.	TPR@5% FPR
Mean Vid-SME	8	2140	0.524	0.530	0.071
		4280	0.531	0.541	0.064
		8560	0.526	0.533	0.043
	16	2140	0.537	0.545	0.078
		4280	0.535	0.540	0.104
		8560	0.539	0.562	0.075
Min_30.0% Vid-SME	8	2140	0.522	0.534	0.050
		4280	0.527	0.538	0.041
		8560	0.538	0.539	0.082
	16	2140	0.548	0.541	0.064
		4280	0.545	0.547	0.074
		8560	0.542	0.545	0.079

Table 4: Performance comparison on different instructions.

Influence of video frame corruptions. The motivation is to detect whether videos are used in training even under potential video corruption. In Figure 4c, we report the attack performance under two different corruptions (Motion Blur and Brightness) at three different levels of corruptions (Marginal, Moderate and Severe). Detailed corruption parameters and examples of the corrupted video frames are given in Appendix B. It can be observed that corrupted video frames make MIAs more difficult, but members can still be detected successfully.

Influence of dataset scales. Table 4 presents the attack performance of Vid-SME on Video-XL-NExT-QA-7B under varying dataset scales. The results show that Vid-SME remains consistently effective as the dataset size increases, demonstrating its scalability.

6 Conclusion

In this work, we investigate the membership inference risk in video understanding large language models (VULLMs). We propose Vid-SME, the first membership inference attack tailored for VULLMs, and self-train three VULLMs for more comprehensive evaluation. Unlike existing methods that fail to capture video-specific temporal dependencies, Vid-SME leverages an adaptive parameterization strategy and both natural and reversed frame sequence to compute the Sharma–Mittal entropy for robust membership signals. Extensive experiments demonstrate the strong effectiveness of Vid-SME.

Acknowledgement

This project is supported by the National Research Foundation, Singapore, and Cyber Security Agency of Singapore under its National Cybersecurity R&D Programme and CyberSG R&D Cyber Research Programme Office (Award: CRPO-GC1-NTU-002).

References

[1] Josh Achiam, Steven Adler, Sandhini Agarwal, Lama Ahmad, Ilge Akkaya, Florencia Leoni Aleman, Diogo Almeida, Janko Altenschmidt, Sam Altman, Shyamal Anadkat, et al. Gpt-4 technical report. *arXiv preprint arXiv:2303.08774*, 2023.

[2] Christian Beck. Generalised information and entropy measures in physics. *Contemporary Physics*, 50(4):495–510, 2009.

[3] Gedas Bertasius, Heng Wang, and Lorenzo Torresani. Is space-time attention all you need for video understanding? In *ICML*, volume 2, page 4, 2021.

[4] Nicholas Carlini, Steve Chien, Milad Nasr, Shuang Song, Andreas Terzis, and Florian Tramer. Membership inference attacks from first principles. In *2022 IEEE symposium on security and privacy (SP)*, pages 1897–1914. IEEE, 2022.

[5] Nicholas Carlini, Chang Liu, Úlfar Erlingsson, Jernej Kos, and Dawn Song. The secret sharer: Evaluating and testing unintended memorization in neural networks. In *28th USENIX security symposium (USENIX security 19)*, pages 267–284, 2019.

[6] Nicholas Carlini, Florian Tramer, Eric Wallace, Matthew Jagielski, Ariel Herbert-Voss, Katherine Lee, Adam Roberts, Tom Brown, Dawn Song, Ulfar Erlingsson, et al. Extracting training data from large language models. In *30th USENIX security symposium (USENIX Security 21)*, pages 2633–2650, 2021.

[7] Wenhao Chai, Enxin Song, Yilun Du, Chenlin Meng, Vashisht Madhavan, Omer Bar-Tal, Jenq-Neng Hwang, Saining Xie, and Christopher D Manning. Auroracap: Efficient, performant video detailed captioning and a new benchmark. *arXiv preprint arXiv:2410.03051*, 2024.

[8] Soravit Changpinyo, Piyush Sharma, Nan Ding, and Radu Soricut. Conceptual 12m: Pushing web-scale image-text pre-training to recognize long-tail visual concepts. In *Proceedings of the IEEE/CVF conference on computer vision and pattern recognition*, pages 3558–3568, 2021.

[9] Moitreya Chatterjee, Narendra Ahuja, and Anoop Cherian. A hierarchical variational neural uncertainty model for stochastic video prediction. In *Proceedings of the IEEE/CVF international conference on computer vision*, pages 9751–9761, 2021.

[10] Dingfan Chen, Ning Yu, Yang Zhang, and Mario Fritz. Gan-leaks: A taxonomy of membership inference attacks against generative models. In *Proceedings of the 2020 ACM SIGSAC conference on computer and communications security*, pages 343–362, 2020.

[11] Lin Chen, Jinsong Li, Xiaoyi Dong, Pan Zhang, Conghui He, Jiaqi Wang, Feng Zhao, and Dahua Lin. Sharegpt4v: Improving large multi-modal models with better captions. In *European Conference on Computer Vision*, pages 370–387. Springer, 2024.

[12] Wei-Lin Chiang, Zhuohan Li, Ziqing Lin, Ying Sheng, Zhanghao Wu, Hao Zhang, Lianmin Zheng, Siyuan Zhuang, Yonghao Zhuang, Joseph E Gonzalez, et al. Vicuna: An open-source chatbot impressing gpt-4 with 90%* chatgpt quality. *See https://vicuna. lmsys. org (accessed 14 April 2023)*, 2(3):6, 2023.

[13] Aakanksha Chowdhery, Sharan Narang, Jacob Devlin, Maarten Bosma, Gaurav Mishra, Adam Roberts, Paul Barham, Hyung Won Chung, Charles Sutton, Sebastian Gehrmann, et al. Palm: Scaling language modeling with pathways. *Journal of Machine Learning Research*, 24(240):1–113, 2023.

[14] Maria Dolores Esteban and Domingo Morales. A summary on entropy statistics. *Kybernetika*, 31(4):337–346, 1995.

[15] Gunnar Farnebäck. *Polynomial expansion for orientation and motion estimation*. Linkopings Universitet (Sweden), 2002.

[16] Yarin Gal and Zoubin Ghahramani. Dropout as a bayesian approximation: Representing model uncertainty in deep learning. In *international conference on machine learning*, pages 1050–1059. PMLR, 2016.

[17] Iryna Hartsock and Ghulam Rasool. Vision-language models for medical report generation and visual question answering: A review. *Frontiers in Artificial Intelligence*, 7:1430984, 2024.

[18] Jamie Hayes, Luca Melis, George Danezis, and Emiliano De Cristofaro. Logan: Membership inference attacks against generative models. *arXiv preprint arXiv:1705.07663*, 2017.

[19] Wenbo Hu, Yifan Xu, Yi Li, Weiyue Li, Zeyuan Chen, and Zhuowen Tu. Bliva: A simple multimodal llm for better handling of text-rich visual questions. In *Proceedings of the AAAI Conference on Artificial Intelligence*, volume 38, pages 2256–2264, 2024.

[20] Yuke Hu, Zheng Li, Zhihao Liu, Yang Zhang, Zhan Qin, Kui Ren, and Chun Chen. Membership inference attacks against vision-language models. *arXiv preprint arXiv:2501.18624*, 2025.

[21] Junnan Li, Dongxu Li, Silvio Savarese, and Steven Hoi. Blip-2: Bootstrapping language-image pre-training with frozen image encoders and large language models. In *International conference on machine learning*, pages 19730–19742. PMLR, 2023.

[22] KunChang Li, Yinan He, Yi Wang, Yizhuo Li, Wenhai Wang, Ping Luo, Yali Wang, Limin Wang, and Yu Qiao. Videochat: Chat-centric video understanding. *arXiv preprint arXiv:2305.06355*, 2023.

[23] Qi Li, Cheng-Long Wang, Yinzhi Cao, and Di Wang. Data lineage inference: Uncovering privacy vulnerabilities of dataset pruning. *arXiv preprint arXiv:2411.15796*, 2024.

[24] Zhan Li, Yongtao Wu, Yihang Chen, Francesco Tonin, Elias Abad Rocamora, and Volkan Cevher. Membership inference attacks against large vision-language models. *Advances in Neural Information Processing Systems*, 37:98645–98674, 2024.

[25] Xiao Lin and Chenliang Xu. Next-qa: Next phase of question answering to explaining temporal actions. In *Proceedings of the IEEE/CVF Conference on Computer Vision and Pattern Recognition (CVPR)*, pages 9777–9786, 2021.

[26] Haotian Liu, Chunyuan Li, Yuheng Li, and Yong Jae Lee. Improved baselines with visual instruction tuning. In *Proceedings of the IEEE/CVF Conference on Computer Vision and Pattern Recognition*, pages 26296–26306, 2024.

[27] Haotian Liu, Chunyuan Li, Yuheng Li, Bo Li, Yuanhan Zhang, Sheng Shen, and Yong Jae Lee. Llava-next: Improved reasoning, ocr, and world knowledge, January 2024.

[28] Ruyang Liu, Chen Li, Haoran Tang, Yixiao Ge, Ying Shan, and Ge Li. St-llm: Large language models are effective temporal learners. In *European Conference on Computer Vision*, pages 1–18. Springer, 2024.

[29] Yuanxin Liu, Shicheng Li, Yi Liu, Yuxiang Wang, Shuhuai Ren, Lei Li, Sishuo Chen, Xu Sun, and Lu Hou. Tempcompass: Do video llms really understand videos? *arXiv preprint arXiv:2403.00476*, 2024.

[30] Muhammad Maaz, Hanoona Rasheed, Salman Khan, and Fahad Shahbaz Khan. Video-chatgpt: Towards detailed video understanding via large vision and language models. *arXiv preprint arXiv:2306.05424*, 2023.

[31] Saeed Mahloujifar, Huseyin A Inan, Melissa Chase, Esha Ghosh, and Marcello Hasegawa. Membership inference on word embedding and beyond. *arXiv preprint arXiv:2106.11384*, 2021.

[32] Salman Khan Muhammad Maaz, Hanoona Rasheed and Fahad Khan. Video-chatgpt: Towards detailed video understanding via large vision and language models. *ArXiv 2306.05424*, 2023.

[33] Bolin Ni, Houwen Peng, Minghao Chen, Songyang Zhang, Gaofeng Meng, Jianlong Fu, Shiming Xiang, and Haibin Ling. Expanding language-image pretrained models for general video recognition. In *European conference on computer vision*, pages 1–18. Springer, 2022.

[34] Ming Nie, Dan Ding, Chunwei Wang, Yuanfan Guo, Jianhua Han, Hang Xu, and Li Zhang. Slowfocus: Enhancing fine-grained temporal understanding in video llm. In *The Thirty-eighth Annual Conference on Neural Information Processing Systems*, 2024.

[35] A Piergiovanni, Chenyou Fan, and Michael Ryoo. Learning latent subevents in activity videos using temporal attention filters. In *Proceedings of the AAAI conference on artificial intelligence*, volume 31, 2017.

[36] Alec Radford, Karthik Narasimhan, Tim Salimans, Ilya Sutskever, et al. Improving language understanding by generative pre-training. 2018.

[37] Hanoona Rasheed, Muhammad Uzair Khattak, Muhammad Maaz, Salman Khan, and Fahad Shahbaz Khan. Fine-tuned clip models are efficient video learners. In *Proceedings of the IEEE/CVF conference on computer vision and pattern recognition*, pages 6545–6554, 2023.

[38] Ruchit Rawal, Khalid Saifullah, Ronen Basri, David Jacobs, Gowthami Somepalli, and Tom Goldstein. Cinepile: A long video question answering dataset and benchmark. *arXiv preprint arXiv:2405.08813*, 2024.

[39] Alfréd Rényi. On measures of entropy and information. In *Proceedings of the fourth Berkeley symposium on mathematical statistics and probability, volume 1: contributions to the theory of statistics*, volume 4, pages 547–562. University of California Press, 1961.

[40] Ahmed Salem, Yang Zhang, Mathias Humbert, Pascal Berrang, Mario Fritz, and Michael Backes. Ml-leaks: Model and data independent membership inference attacks and defenses on machine learning models. *arXiv preprint arXiv:1806.01246*, 2018.

[41] Claude E Shannon. A mathematical theory of communication. *The Bell system technical journal*, 27(3):379–423, 1948.

[42] Bhudev D Sharma and Dharam P Mittal. New non-additive measures of entropy for discrete probability distributions. *J. Math. Sci*, 10(75):28–40, 1975.

[43] Weijia Shi, Anirudh Ajith, Mengzhou Xia, Yangsibo Huang, Daogao Liu, Terra Blevins, Danqi Chen, and Luke Zettlemoyer. Detecting pretraining data from large language models. *arXiv preprint arXiv:2310.16789*, 2023.

[44] Reza Shokri, Marco Stronati, Congzheng Song, and Vitaly Shmatikov. Membership inference attacks against machine learning models. In *2017 IEEE symposium on security and privacy (SP)*, pages 3–18. IEEE, 2017.

[45] Yan Shu, Peitian Zhang, Zheng Liu, Minghao Qin, Junjie Zhou, Tiejun Huang, and Bo Zhao. Video-xl: Extra-long vision language model for hour-scale video understanding. *arXiv preprint arXiv:2409.14485*, 2024.

[46] Karen Simonyan and Andrew Zisserman. Two-stream convolutional networks for action recognition in videos. *Advances in neural information processing systems*, 27, 2014.

[47] Congzheng Song and Ananth Raghunathan. Information leakage in embedding models. In *Proceedings of the 2020 ACM SIGSAC conference on computer and communications security*, pages 377–390, 2020.

[48] Congzheng Song, Thomas Ristenpart, and Vitaly Shmatikov. Machine learning models that remember too much. In *Proceedings of the 2017 ACM SIGSAC Conference on computer and communications security*, pages 587–601, 2017.

[49] Liwei Song and Prateek Mittal. Systematic evaluation of privacy risks of machine learning models. In *30th USENIX Security Symposium (USENIX Security 21)*, pages 2615–2632, 2021.

[50] Liwei Song, Reza Shokri, and Prateek Mittal. Membership inference attacks against adversarially robust deep learning models. In *2019 IEEE Security and Privacy Workshops (SPW)*, pages 50–56. IEEE, 2019.

[51] Inder Jeet Taneja. On generalized information measures and their applications. In *Advances in Electronics and Electron Physics*, volume 76, pages 327–413. Elsevier, 1989.

[52] Hugo Touvron, Louis Martin, Kevin Stone, Peter Albert, Amjad Almahairi, Yasmine Babaei, Nikolay Bashlykov, Soumya Batra, Prajjwal Bhargava, Shruti Bhosale, et al. Llama 2: Open foundation and fine-tuned chat models. *arXiv preprint arXiv:2307.09288*, 2023.

[53] Constantino Tsallis. Possible generalization of boltzmann-gibbs statistics. *Journal of statistical physics*, 52:479–487, 1988.

[54] Cheng-Long Wang, Qi Li, Zihang Xiang, Yinzhi Cao, and Di Wang. Towards lifecycle unlearning commitment management: Measuring sample-level approximate unlearning completeness. *arXiv preprint arXiv:2403.12830*, 2024.

[55] Weihan Wang, Qingsong Lv, Wenmeng Yu, Wenyi Hong, Ji Qi, Yan Wang, Junhui Ji, Zhuoyi Yang, Lei Zhao, Song XiXuan, et al. Cogvlm: Visual expert for pretrained language models. *Advances in Neural Information Processing Systems*, 37:121475–121499, 2024.

[56] Xiaohan Wang, Yuhui Zhang, Orr Zohar, and Serena Yeung-Levy. Videoagent: Long-form video understanding with large language model as agent. In *European Conference on Computer Vision*, pages 58–76. Springer, 2024.

[57] Hengyu Wu and Yang Cao. Membership inference attacks on large-scale models: A survey. *arXiv preprint arXiv:2503.19338*, 2025.

[58] Yue Wu, Qiang Wen, and Qifeng Chen. Optimizing video prediction via video frame interpolation. In *Proceedings of the IEEE/CVF Conference on Computer Vision and Pattern Recognition*, pages 17814–17823, 2022.

[59] Samuel Yeom, Irene Giacomelli, Matt Fredrikson, and Somesh Jha. Privacy risk in machine learning: Analyzing the connection to overfitting. In *2018 IEEE 31st computer security foundations symposium (CSF)*, pages 268–282. IEEE, 2018.

[60] Sajjad Zarifzadeh, Philippe Liu, and Reza Shokri. Low-cost high-power membership inference attacks. *arXiv preprint arXiv:2312.03262*, 2023.

[61] Chiyuan Zhang, Samy Bengio, Moritz Hardt, Benjamin Recht, and Oriol Vinyals. Understanding deep learning (still) requires rethinking generalization. *Communications of the ACM*, 64(3):107–115, 2021.

[62] Jingyang Zhang, Jingwei Sun, Eric Yeats, Yang Ouyang, Martin Kuo, Jianyi Zhang, Hao Frank Yang, and Hai Li. Min-k%++: Improved baseline for detecting pre-training data from large language models. *arXiv preprint arXiv:2404.02936*, 2024.

[63] Peiyuan Zhang, Kaichen Zhang, Bo Li, Guangtao Zeng, Jingkang Yang, Yuanhan Zhang, Ziyue Wang, Haoran Tan, Chunyuan Li, and Ziwei Liu. Long context transfer from language to vision. *arXiv preprint arXiv:2406.16852*, 2024.

[64] Shengyu Zhang, Linfeng Dong, Xiaoya Li, Sen Zhang, Xiaofei Sun, Shuhe Wang, Jiwei Li, Runyi Hu, Tianwei Zhang, Fei Wu, et al. Instruction tuning for large language models: A survey. *arXiv preprint arXiv:2308.10792*, 2023.

[65] Yuanhan Zhang, Bo Li, haotian Liu, Yong jae Lee, Liangke Gui, Di Fu, Jiashi Feng, Ziwei Liu, and Chunyuan Li. Llava-next: A strong zero-shot video understanding model, April 2024.

[66] Junjie Zhou, Yan Shu, Bo Zhao, Boya Wu, Shitao Xiao, Xi Yang, Yongping Xiong, Bo Zhang, Tiejun Huang, and Zheng Liu. Mlvu: A comprehensive benchmark for multi-task long video understanding. *arXiv preprint arXiv:2406.04264*, 2024.

[67] Tianfei Zhou, Fatih Porikli, David J Crandall, Luc Van Gool, and Wenguan Wang. A survey on deep learning technique for video segmentation. *IEEE transactions on pattern analysis and machine intelligence*, 45(6):7099–7122, 2022.

A Model Configurations and Training States

We report the model configurations of the three self-trained VULLMs in Table 5, and the training loss and gradient norm over steps in Figure 7.

Field	**Video-XL-NExT-QA-7B**	**Video-XL-CinePile-7B**	**LongVA-Caption-7B**
Base LLM	Qwen2-7B-Instruct-224K	Qwen2-7B-Instruct-224K	Qwen2-7B-Instruct-224K
bos_token_id	151643	151643	151643
eos_token_id	151645	151645	151645
Hidden Activation	silu	silu	silu
Resampler type	spatial_pool	spatial_pool	spatial_pool
Vision tower	clip-vit-large-patch14-336	clip-vit-large-patch14-336	clip-vit-large-patch14-336
Vision tower lr	2e-6	2e-6	2e-6
Max window layers	28	28	28
Projector type	mlp2x_gelu	mlp2x_gelu	mlp2x_gelu
#Heads	28	28	28
#Hidden Layers	28	28	28
KV heads	4	4	4
Tokenizer padding side	right	right	right
Vocab size	152064	152064	152064
Added tokens	<|endoftext|>: 151643 <|im_end|>: 151645 <|im_start|>: 151644	<|endoftext|>: 151643 <|im_end|>: 151645 <|im_start|>: 151644	<|endoftext|>: 151643 <|im_end|>: 151645 <|im_start|>: 151644
Special tokens map	pad_token: <|endoftext|> eos_token: <|im_end|>	pad_token: <|endoftext|> eos_token: <|im_end|>	pad_token: <|endoftext|> eos_token: <|im_end|>

Table 5: Model configurations of the three self-trained models.

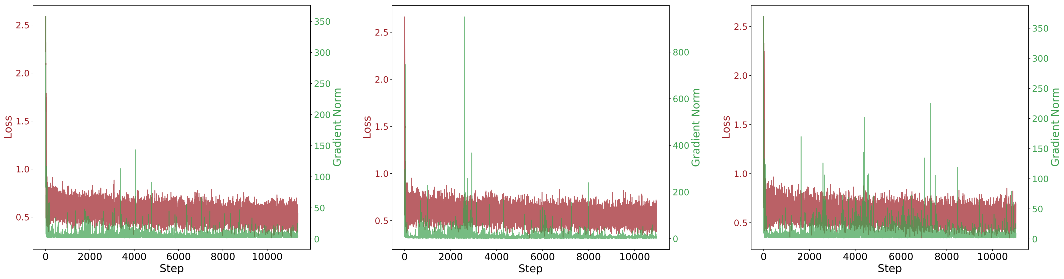

(a) Video-XL-NExT-QA-7B (b) Video-XL-CinePile-7B (c) LongVA-Caption-7B

Figure 7: Training Loss and Gradient Norm over Steps for the three self-trained models.

B Examples of the Video-Text Instruction Context

In Figure 8, we give an example of the video-text instruction context used in our experiments. In addition, we also provide the corrupted video frames under different types and levels of corruptions in Figure 8. The details of the parameters of different corruptions are given in Table 6. Specifically, for brightness corruption, we adjust the pixel intensity by randomly adding/subtracting a constant value of 20, 60, and 100 for marginal, moderate, and severe conditions, respectively. For motion blur, we apply a convolutional kernel with size and angle parameters set to (10, 5), (15, 5), and (20, 10) to simulate increasing degrees of blur under the same three corruption levels.

	Brightness	Motion Blur
Marginal	20	(10,5)
Moderate	60	(15,5)
Severe	100	(20,10)

Table 6: Brightness and Motion Blur Levels under Different Conditions.

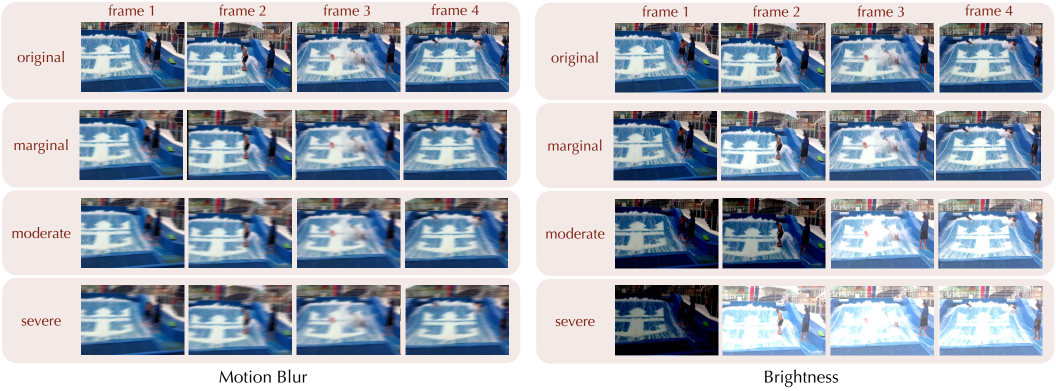

system:
Carefully watch this video and pay attention to every detail. Based on your observations, select the best option that accurately addresses the question.
user:
<video>
Question: Why did the man moved upwards after he fell down?
Options:
(A) change posture to support baby (B) blocked by pumpkin (C) snow blocking him (D) pushed by water (E) moving the cardboard backwards
Only give the best option.
assistant:
Best Option:

Figure 8: Example of the video-text instruction context under different types and levels of corruptions.

system:
Carefully watch this video and pay attention to every detail. Based on your observations, select the best option that accurately addresses the question.
user:
<video>...
assistant:
Best Option: I_1

system:
You will be shown a video. Examine it carefully and use all visual cues to determine the correct answer. Your response should be the most accurate option.
user:
<video>...
assistant:
The correct answer is: I_2

system:
You're going to see a video. Take a good look and try to understand what's going on. Based on that, help pick the option that makes the most sense.
user:
<video>...
assistant:
I think the best choice is: I_3

Figure 9: The three different instruction contexts used in the ablation study.

system:
You are a helpful assistant.
user:
<video>
Describe this video in detail.
assistant:
Response:

Figure 10: The short query text used in the ablation study.

C Different Instructions Used in the Ablation Study.

We give the contents of the three different instructions used in the ablation study in Figure 9. The short query text used in the ablation study is given in Figure 10.

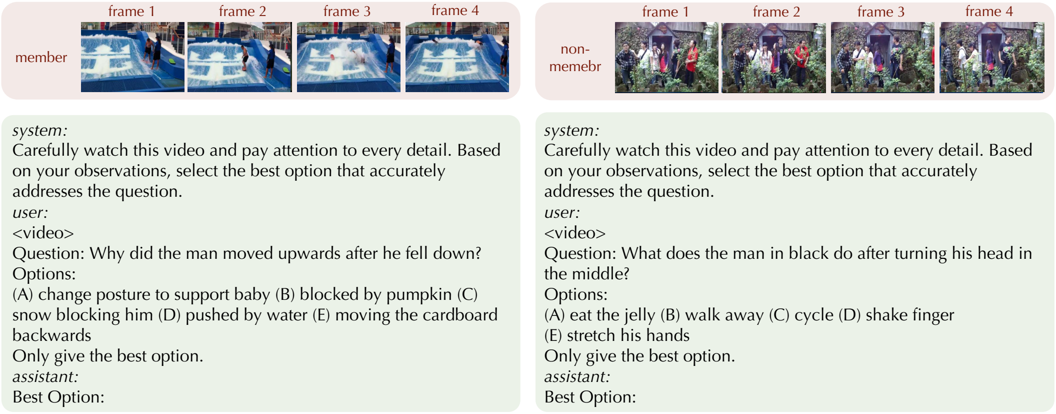

system:
Carefully watch this video and pay attention to every detail. Based on your observations, select the best option that accurately addresses the question.
user:
<video>
Question: Why did the man moved upwards after he fell down?
Options:
(A) change posture to support baby (B) blocked by pumpkin (C) snow blocking him (D) pushed by water (E) moving the cardboard backwards
Only give the best option.
assistant:
Best Option:

system:
Carefully watch this video and pay attention to every detail. Based on your observations, select the best option that accurately addresses the question.
user:
<video>
Question: What does the man in black do after turning his head in the middle?
Options:
(A) eat the jelly (B) walk away (C) cycle (D) shake finger
(E) stretch his hands
Only give the best option.
assistant:
Best Option:

Figure 11: An example of member and non-member data for Video-XL-NExT-QA-7B.

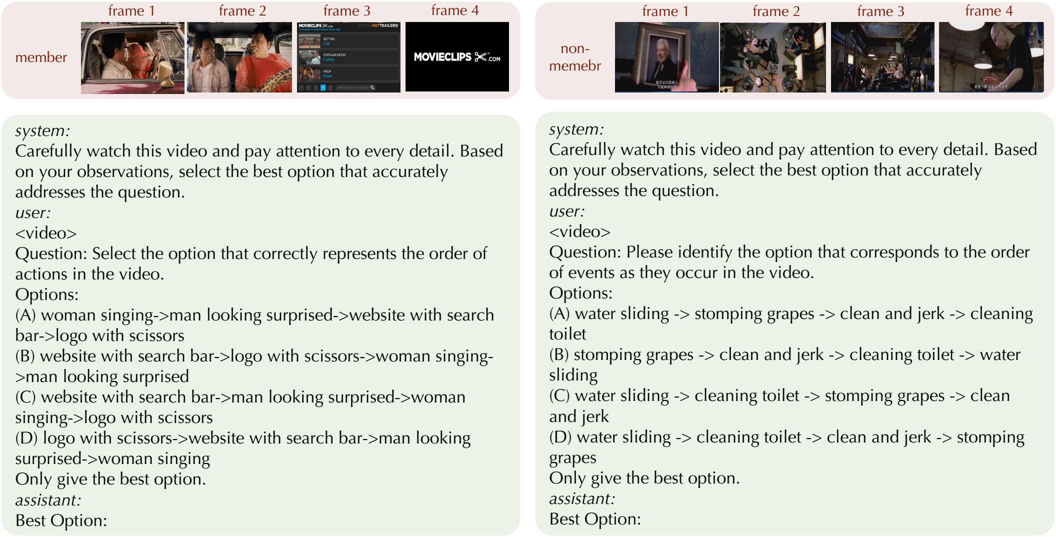

system:
Carefully watch this video and pay attention to every detail. Based on your observations, select the best option that accurately addresses the question.
user:
<video>
Question: Select the option that correctly represents the order of actions in the video.
Options:
(A) woman singing->man looking surprised->website with search bar->logo with scissors
(B) website with search bar->logo with scissors->woman singing->man looking surprised
(C) website with search bar->man looking surprised->woman singing->logo with scissors
(D) logo with scissors->website with search bar->man looking surprised->woman singing
Only give the best option.
assistant:
Best Option:

system:
Carefully watch this video and pay attention to every detail. Based on your observations, select the best option that accurately addresses the question.
user:
<video>
Question: Please identify the option that corresponds to the order of events as they occur in the video.
Options:
(A) water sliding -> stomping grapes -> clean and jerk -> cleaning toilet
(B) stomping grapes -> clean and jerk -> cleaning toilet -> water sliding
(C) water sliding -> cleaning toilet -> stomping grapes -> clean and jerk
(D) water sliding -> cleaning toilet -> clean and jerk -> stomping grapes
Only give the best option.
assistant:
Best Option:

Figure 12: An example of member and non-member data for Video-XL-CinePile-7B.

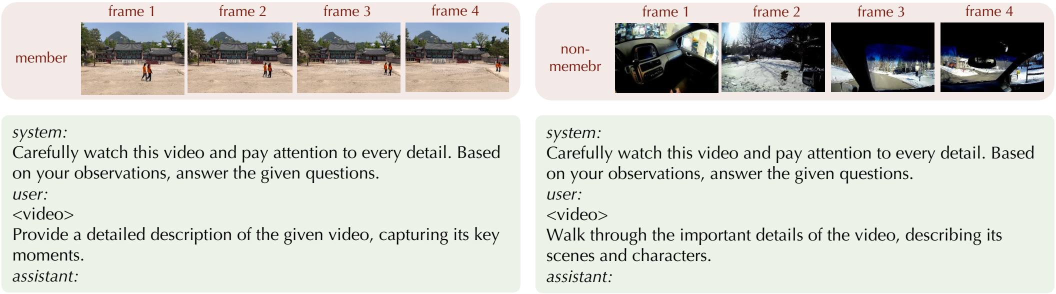

system:
Carefully watch this video and pay attention to every detail. Based on your observations, answer the given questions.
user:
<video>
Provide a detailed description of the given video, capturing its key moments.
assistant:

system:
Carefully watch this video and pay attention to every detail. Based on your observations, answer the given questions.
user:
<video>
Walk through the important details of the video, describing its scenes and characters.
assistant:

Figure 13: An example of member and non-member data for Longva-Caption-7B.

D Computation resource usage.

The three self-trained models are trained on 8 A100 GPUs, while all experiments are conducted using 8 NVIDIA RTX A5000 GPUs.

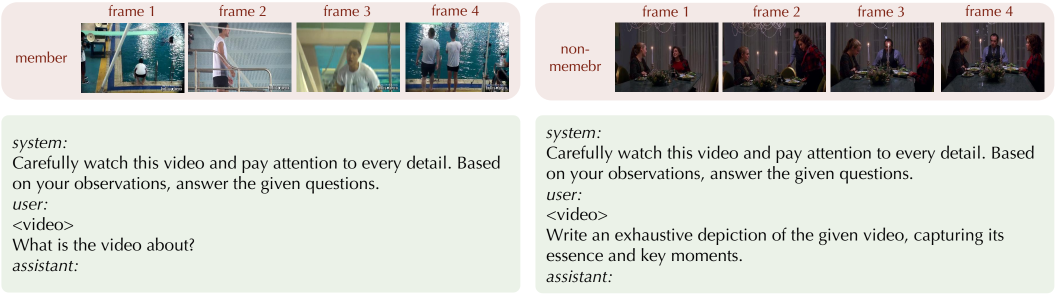

system:
Carefully watch this video and pay attention to every detail. Based on your observations, answer the given questions.
user:
<video>
What is the video about?
assistant:

system:
Carefully watch this video and pay attention to every detail. Based on your observations, answer the given questions.
user:
<video>
Write an exhaustive depiction of the given video, capturing its essence and key moments.
assistant:

Figure 14: An example of member and non-member data for LLaVA-NeXT-Video-7B/34B.

E Examples of Members and Non-Members of the Target Models.

We give examples of members and non-members of the five target models used in our experiments in Figures 11, 12, 13, 14.

F Simplified Terms of Sharma–Mittal Entropy

The Sharma–Mittal entropy for a probability distribution $p = \{p_i\}$ is defined as:

$$S_{q,r}(p) = \frac{1}{1-r}\left[\left(\sum_i p_i^q\right)^{\frac{1-r}{1-q}} - 1\right], \tag{5}$$

where q controls the sensitivity to distribution skewness, and r determines the nonlinearity of aggregation. This generalized formulation subsumes several classical entropy measures as special cases. We give the formal definitions as follows:

F.1 Reduction to Shannon Entropy

As both $q \to 1$ and $r \to 1$, Equation (5) reduces to Shannon entropy:

$$\lim_{q\to 1, r\to 1} S_{q,r}(p) = -\sum_i p_i \log p_i. \tag{6}$$

This limit follows from applying L'Hôpital's Rule to both the exponent and denominator as $q \to 1$ and $r \to 1$.

F.2 Reduction to Rényi Entropy

When $r \to 1$ and $q \neq 1$, Equation (5) simplifies to the Rényi entropy:

$$\lim_{r\to 1} S_{q,r}(p) = \frac{1}{1-q}\log\sum_i p_i^q. \tag{7}$$

F.3 Reduction to Tsallis Entropy

When $r = q$, Equation (5) reduces to the Tsallis entropy:

$$S_{q,q}(p) = \frac{1}{1-q}\left(\sum_i p_i^q - 1\right). \tag{8}$$

These reductions demonstrate that Sharma–Mittal entropy serves as a unified framework encompassing Shannon, Rényi, and Tsallis entropies as limiting cases.

G Broader Impact

This work explores the privacy vulnerabilities of Video Understanding Large Language Models (VULLMs) through membership inference attacks (MIAs), revealing how sensitive training data can be partially reconstructed or identified from model behavior.

G.1 Positive Societal Impacts

Our study contributes to the broader goal of trustworthy multimodal AI by uncovering potential privacy risks before such models are widely deployed. The insights and benchmark we introduce can inform defensive research, such as differential privacy mechanisms, data sanitization, and auditing protocols, helping model developers detect and mitigate leakage risks in future VLM releases. Moreover, the framework provides a systematic methodology for assessing privacy robustness in multimodal systems, filling a critical gap between vision and language privacy research.

G.2 Negative Social Impact

At the same time, the attack methods demonstrated in this paper could, if misused, be exploited to extract private or copyrighted visual content from proprietary VLMs. Although our experiments are conducted under controlled academic settings, similar approaches might be repurposed for malicious data mining or surveillance.

NeurIPS Paper Checklist

1. **Claims**

   Question: Do the main claims made in the abstract and introduction accurately reflect the paper's contributions and scope?

   Answer: [Yes]

   Justification: The main claims in the abstract and introduction accurately reflect our contributions.

   Guidelines:

   - The answer NA means that the abstract and introduction do not include the claims made in the paper.
   - The abstract and/or introduction should clearly state the claims made, including the contributions made in the paper and important assumptions and limitations. A No or NA answer to this question will not be perceived well by the reviewers.
   - The claims made should match theoretical and experimental results, and reflect how much the results can be expected to generalize to other settings.
   - It is fine to include aspirational goals as motivation as long as it is clear that these goals are not attained by the paper.

2. **Limitations**

   Question: Does the paper discuss the limitations of the work performed by the authors?

   Answer: [Yes]

   Justification:The limitations are given in the supplementary material.

   Guidelines:

   - The answer NA means that the paper has no limitation while the answer No means that the paper has limitations, but those are not discussed in the paper.
   - The authors are encouraged to create a separate "Limitations" section in their paper.
   - The paper should point out any strong assumptions and how robust the results are to violations of these assumptions (e.g., independence assumptions, noiseless settings, model well-specification, asymptotic approximations only holding locally). The authors should reflect on how these assumptions might be violated in practice and what the implications would be.
   - The authors should reflect on the scope of the claims made, e.g., if the approach was only tested on a few datasets or with a few runs. In general, empirical results often depend on implicit assumptions, which should be articulated.
   - The authors should reflect on the factors that influence the performance of the approach. For example, a facial recognition algorithm may perform poorly when image resolution is low or images are taken in low lighting. Or a speech-to-text system might not be used reliably to provide closed captions for online lectures because it fails to handle technical jargon.
   - The authors should discuss the computational efficiency of the proposed algorithms and how they scale with dataset size.
   - If applicable, the authors should discuss possible limitations of their approach to address problems of privacy and fairness.
   - While the authors might fear that complete honesty about limitations might be used by reviewers as grounds for rejection, a worse outcome might be that reviewers discover limitations that aren't acknowledged in the paper. The authors should use their best judgment and recognize that individual actions in favor of transparency play an important role in developing norms that preserve the integrity of the community. Reviewers will be specifically instructed to not penalize honesty concerning limitations.

3. **Theory assumptions and proofs**

   Question: For each theoretical result, does the paper provide the full set of assumptions and a complete (and correct) proof?

   Answer: [NA]

Justification: The paper does not include theoretical results.

Guidelines:

- The answer NA means that the paper does not include theoretical results.
- All the theorems, formulas, and proofs in the paper should be numbered and cross-referenced.
- All assumptions should be clearly stated or referenced in the statement of any theorems.
- The proofs can either appear in the main paper or the supplemental material, but if they appear in the supplemental material, the authors are encouraged to provide a short proof sketch to provide intuition.
- Inversely, any informal proof provided in the core of the paper should be complemented by formal proofs provided in appendix or supplemental material.
- Theorems and Lemmas that the proof relies upon should be properly referenced.

4. **Experimental result reproducibility**

   Question: Does the paper fully disclose all the information needed to reproduce the main experimental results of the paper to the extent that it affects the main claims and/or conclusions of the paper (regardless of whether the code and data are provided or not)?

   Answer: [Yes]

   Justification: Useful information related to reproduce the results are given in the paper and the supplementary material.

   Guidelines:

   - The answer NA means that the paper does not include experiments.
   - If the paper includes experiments, a No answer to this question will not be perceived well by the reviewers: Making the paper reproducible is important, regardless of whether the code and data are provided or not.
   - If the contribution is a dataset and/or model, the authors should describe the steps taken to make their results reproducible or verifiable.
   - Depending on the contribution, reproducibility can be accomplished in various ways. For example, if the contribution is a novel architecture, describing the architecture fully might suffice, or if the contribution is a specific model and empirical evaluation, it may be necessary to either make it possible for others to replicate the model with the same dataset, or provide access to the model. In general. releasing code and data is often one good way to accomplish this, but reproducibility can also be provided via detailed instructions for how to replicate the results, access to a hosted model (e.g., in the case of a large language model), releasing of a model checkpoint, or other means that are appropriate to the research performed.
   - While NeurIPS does not require releasing code, the conference does require all submissions to provide some reasonable avenue for reproducibility, which may depend on the nature of the contribution. For example
     (a) If the contribution is primarily a new algorithm, the paper should make it clear how to reproduce that algorithm.
     (b) If the contribution is primarily a new model architecture, the paper should describe the architecture clearly and fully.
     (c) If the contribution is a new model (e.g., a large language model), then there should either be a way to access this model for reproducing the results or a way to reproduce the model (e.g., with an open-source dataset or instructions for how to construct the dataset).
     (d) We recognize that reproducibility may be tricky in some cases, in which case authors are welcome to describe the particular way they provide for reproducibility. In the case of closed-source models, it may be that access to the model is limited in some way (e.g., to registered users), but it should be possible for other researchers to have some path to reproducing or verifying the results.

5. **Open access to data and code**

   Question: Does the paper provide open access to the data and code, with sufficient instructions to faithfully reproduce the main experimental results, as described in supplemental material?

Answer: [Yes]

Justification: The code is made public available here.

Guidelines:

- The answer NA means that paper does not include experiments requiring code.
- Please see the NeurIPS code and data submission guidelines (`https://nips.cc/public/guides/CodeSubmissionPolicy`) for more details.
- While we encourage the release of code and data, we understand that this might not be possible, so "No" is an acceptable answer. Papers cannot be rejected simply for not including code, unless this is central to the contribution (e.g., for a new open-source benchmark).
- The instructions should contain the exact command and environment needed to run to reproduce the results. See the NeurIPS code and data submission guidelines (`https://nips.cc/public/guides/CodeSubmissionPolicy`) for more details.
- The authors should provide instructions on data access and preparation, including how to access the raw data, preprocessed data, intermediate data, and generated data, etc.
- The authors should provide scripts to reproduce all experimental results for the new proposed method and baselines. If only a subset of experiments are reproducible, they should state which ones are omitted from the script and why.
- At submission time, to preserve anonymity, the authors should release anonymized versions (if applicable).
- Providing as much information as possible in supplemental material (appended to the paper) is recommended, but including URLs to data and code is permitted.

6. **Experimental setting/details**

   Question: Does the paper specify all the training and test details (e.g., data splits, hyperparameters, how they were chosen, type of optimizer, etc.) necessary to understand the results?

   Answer: [Yes]

   Justification: The experimental details are provided.

   Guidelines:

   - The answer NA means that the paper does not include experiments.
   - The experimental setting should be presented in the core of the paper to a level of detail that is necessary to appreciate the results and make sense of them.
   - The full details can be provided either with the code, in appendix, or as supplemental material.

7. **Experiment statistical significance**

   Question: Does the paper report error bars suitably and correctly defined or other appropriate information about the statistical significance of the experiments?

   Answer: [Yes]

   Justification: The experimental section presents results under identical settings with different relevant parameters.

   Guidelines:

   - The answer NA means that the paper does not include experiments.
   - The authors should answer "Yes" if the results are accompanied by error bars, confidence intervals, or statistical significance tests, at least for the experiments that support the main claims of the paper.
   - The factors of variability that the error bars are capturing should be clearly stated (for example, train/test split, initialization, random drawing of some parameter, or overall run with given experimental conditions).
   - The method for calculating the error bars should be explained (closed form formula, call to a library function, bootstrap, etc.)
   - The assumptions made should be given (e.g., Normally distributed errors).

- It should be clear whether the error bar is the standard deviation or the standard error of the mean.
- It is OK to report 1-sigma error bars, but one should state it. The authors should preferably report a 2-sigma error bar than state that they have a 96% CI, if the hypothesis of Normality of errors is not verified.
- For asymmetric distributions, the authors should be careful not to show in tables or figures symmetric error bars that would yield results that are out of range (e.g. negative error rates).
- If error bars are reported in tables or plots, The authors should explain in the text how they were calculated and reference the corresponding figures or tables in the text.

8. **Experiments compute resources**

   Question: For each experiment, does the paper provide sufficient information on the computer resources (type of compute workers, memory, time of execution) needed to reproduce the experiments?

   Answer: [Yes]

   Justification: Detials are provided in the supplementary material.

   Guidelines:

   - The answer NA means that the paper does not include experiments.
   - The paper should indicate the type of compute workers CPU or GPU, internal cluster, or cloud provider, including relevant memory and storage.
   - The paper should provide the amount of compute required for each of the individual experimental runs as well as estimate the total compute.
   - The paper should disclose whether the full research project required more compute than the experiments reported in the paper (e.g., preliminary or failed experiments that didn't make it into the paper).

9. **Code of ethics**

   Question: Does the research conducted in the paper conform, in every respect, with the NeurIPS Code of Ethics `https://neurips.cc/public/EthicsGuidelines`?

   Answer: [Yes]

   Justification: The paper conform, in every respect, with the NeurIPS Code of Ethics.

   Guidelines:

   - The answer NA means that the authors have not reviewed the NeurIPS Code of Ethics.
   - If the authors answer No, they should explain the special circumstances that require a deviation from the Code of Ethics.
   - The authors should make sure to preserve anonymity (e.g., if there is a special consideration due to laws or regulations in their jurisdiction).

10. **Broader impacts**

    Question: Does the paper discuss both potential positive societal impacts and negative societal impacts of the work performed?

    Answer: [Yes]

    Justification: Detailed discussions are given in the supplementary material.

    Guidelines:

    - The answer NA means that there is no societal impact of the work performed.
    - If the authors answer NA or No, they should explain why their work has no societal impact or why the paper does not address societal impact.
    - Examples of negative societal impacts include potential malicious or unintended uses (e.g., disinformation, generating fake profiles, surveillance), fairness considerations (e.g., deployment of technologies that could make decisions that unfairly impact specific groups), privacy considerations, and security considerations.

- The conference expects that many papers will be foundational research and not tied to particular applications, let alone deployments. However, if there is a direct path to any negative applications, the authors should point it out. For example, it is legitimate to point out that an improvement in the quality of generative models could be used to generate deepfakes for disinformation. On the other hand, it is not needed to point out that a generic algorithm for optimizing neural networks could enable people to train models that generate Deepfakes faster.
- The authors should consider possible harms that could arise when the technology is being used as intended and functioning correctly, harms that could arise when the technology is being used as intended but gives incorrect results, and harms following from (intentional or unintentional) misuse of the technology.
- If there are negative societal impacts, the authors could also discuss possible mitigation strategies (e.g., gated release of models, providing defenses in addition to attacks, mechanisms for monitoring misuse, mechanisms to monitor how a system learns from feedback over time, improving the efficiency and accessibility of ML).

11. **Safeguards**

    Question: Does the paper describe safeguards that have been put in place for responsible release of data or models that have a high risk for misuse (e.g., pretrained language models, image generators, or scraped datasets)?

    Answer: [NA]

    Justification: The paper poses no such risks.

    Guidelines:

    - The answer NA means that the paper poses no such risks.
    - Released models that have a high risk for misuse or dual-use should be released with necessary safeguards to allow for controlled use of the model, for example by requiring that users adhere to usage guidelines or restrictions to access the model or implementing safety filters.
    - Datasets that have been scraped from the Internet could pose safety risks. The authors should describe how they avoided releasing unsafe images.
    - We recognize that providing effective safeguards is challenging, and many papers do not require this, but we encourage authors to take this into account and make a best faith effort.

12. **Licenses for existing assets**

    Question: Are the creators or original owners of assets (e.g., code, data, models), used in the paper, properly credited and are the license and terms of use explicitly mentioned and properly respected?

    Answer: [Yes]

    Justification: We cite the original paper that produced the code package or dataset.

    Guidelines:

    - The answer NA means that the paper does not use existing assets.
    - The authors should cite the original paper that produced the code package or dataset.
    - The authors should state which version of the asset is used and, if possible, include a URL.
    - The name of the license (e.g., CC-BY 4.0) should be included for each asset.
    - For scraped data from a particular source (e.g., website), the copyright and terms of service of that source should be provided.
    - If assets are released, the license, copyright information, and terms of use in the package should be provided. For popular datasets, `paperswithcode.com/datasets` has curated licenses for some datasets. Their licensing guide can help determine the license of a dataset.
    - For existing datasets that are re-packaged, both the original license and the license of the derived asset (if it has changed) should be provided.

- If this information is not available online, the authors are encouraged to reach out to the asset's creators.

13. **New assets**

    Question: Are new assets introduced in the paper well documented and is the documentation provided alongside the assets?

    Answer: [Yes]

    Justification: The new assets introduced are made public available here.

    Guidelines:

    - The answer NA means that the paper does not release new assets.
    - Researchers should communicate the details of the dataset/code/model as part of their submissions via structured templates. This includes details about training, license, limitations, etc.
    - The paper should discuss whether and how consent was obtained from people whose asset is used.
    - At submission time, remember to anonymize your assets (if applicable). You can either create an anonymized URL or include an anonymized zip file.

14. **Crowdsourcing and research with human subjects**

    Question: For crowdsourcing experiments and research with human subjects, does the paper include the full text of instructions given to participants and screenshots, if applicable, as well as details about compensation (if any)?

    Answer: [NA]

    Justification: The paper does not involve crowdsourcing nor research with human subjects.

    Guidelines:

    - The answer NA means that the paper does not involve crowdsourcing nor research with human subjects.
    - Including this information in the supplemental material is fine, but if the main contribution of the paper involves human subjects, then as much detail as possible should be included in the main paper.
    - According to the NeurIPS Code of Ethics, workers involved in data collection, curation, or other labor should be paid at least the minimum wage in the country of the data collector.

15. **Institutional review board (IRB) approvals or equivalent for research with human subjects**

    Question: Does the paper describe potential risks incurred by study participants, whether such risks were disclosed to the subjects, and whether Institutional Review Board (IRB) approvals (or an equivalent approval/review based on the requirements of your country or institution) were obtained?

    Answer: [NA]

    Justification: The paper does not involve crowdsourcing nor research with human subjects.

    Guidelines:

    - The answer NA means that the paper does not involve crowdsourcing nor research with human subjects.
    - Depending on the country in which research is conducted, IRB approval (or equivalent) may be required for any human subjects research. If you obtained IRB approval, you should clearly state this in the paper.
    - We recognize that the procedures for this may vary significantly between institutions and locations, and we expect authors to adhere to the NeurIPS Code of Ethics and the guidelines for their institution.
    - For initial submissions, do not include any information that would break anonymity (if applicable), such as the institution conducting the review.

16. **Declaration of LLM usage**

Question: Does the paper describe the usage of LLMs if it is an important, original, or non-standard component of the core methods in this research? Note that if the LLM is used only for writing, editing, or formatting purposes and does not impact the core methodology, scientific rigorousness, or originality of the research, declaration is not required.

Answer: [NA]

Justification: The core method development in this research does not involve LLMs as any important, original, or non-standard components.

Guidelines:

- The answer NA means that the core method development in this research does not involve LLMs as any important, original, or non-standard components.
- Please refer to our LLM policy (`https://neurips.cc/Conferences/2025/LLM`) for what should or should not be described.